Domain II plays a crucial role in the function of ribosome recycling factor

Peng GUO[1], Liqiang ZHANG[1], Hongjie ZHANG, Yanming FENG and Guozhong JING[2]

National Laboratory of Biomacromolecules, Institute of Biophysics, Chinese Academy of Sciences, 15 Datun Rd., Chaoyang District, Beijing 100101, China

RRF (ribosome recycling factor) consists of two domains, and in concert with EF-G (elongation factor-G), triggers dissociation of the post-termination ribosomal complex. However, the function of the individual domains of RRF remains unclear. To clarify this, two RRF chimaeras, *Eco*DI/*Tte*DII and *Tte*DI/*Eco*DII, were created by domain swaps between the proteins from *Escherichia coli* and *Thermoanaerobacter tengcongensis*. The ribosome recycling activity of the RRF chimaeras was compared with their wild-type RRFs by using *in vivo* and *in vitro* activity assays. Like wild-type *Tte*RRF (*T. tengcongensis* RRF), the *Eco*DI/*Tte*DII chimaera is non-functional in *E. coli*, but both wild-type *Tte*RRF, and *Eco*DI/*Tte*DII can be activated by coexpression of *T. tengcongensis* EF-G in *E. coli*. By contrast, like wild-type *E. coli* RRF (*Eco*RRF), *Tte*DI/*Eco*DII is fully functional in *E. coli*. These findings suggest that domain II of RRF plays a crucial role in the concerted action of RRF and EF-G for the post-termination complex disassembly, and the specific interaction between RRF and EF-G on ribosomes mainly depends on the interaction between domain II of RRF and EF-G. This study provides direct genetic and biochemical evidence for the function of the individual domains of RRF.

Key words: domain function, domain swaps, *Escherichia coli*, elongation factor (EF-G), ribosome recycling factor (RRF), *Thermoanaerobacter tengcongensis*.

INTRODUCTION

Protein synthesis consists of initiation, elongation, termination and ribosome recycling. When translation of an mRNA has been completed on the ribosome, the peptidyl-tRNA with a nascent polypeptide is translocated into the ribosomal P site, and a stop codon is translocated into the ribosomal A site. Then either class I RF1 (release factor1) or RF2 binds to the ribosomal A site and induces the release of the nascent polypeptide. Afterwards class II RF3 binds to the ribosome, catalyses the release of RF1 or RF2, and dissociates in a GTP-dependent manner [1–3], leaving behind the post-termination ribosomal complex consisting of mRNA, deacylated tRNA in the P site, and an empty A site. Disassembly of the post-termination complex, and recycling of the ribosomal subunits back to a new round of initiation, is an essential step in protein synthesis, which is catalysed by RRF (ribosome recycling factor) and EF-G (elongation factor-G) [4–7]. Although the simplest explanation that RRF is a functional mimic of tRNA for disassembly of the post-termination complex has been ruled out [8–10], the mechanism of ribosomal recycling is still a debated issue. One point of dispute is whether disassembly of the post-termination complex depends on the translocation activity of EF-G. Kiel et al. demonstrated that, as part of the RRF-dependent post-termination complex disassembly reaction, EF-G released RRF from ribosomal complexes, and this release activity of EF-G was due to the translocation activity of EF-G [11]. By contrast, Fujiwara et al. pointed out that RRF disassembled the post-termination ribosomal complex independently of the ribosomal translocase activity of EF-G, based on the results showing that EF-G variants remain active in GTP hydrolysis but are defective in tRNA translocation fully activate RRF function *in vivo* and *in vitro* [10]. Recently, by using fluorescence and fluorescence resonance energy transfer assays to monitor sequence of steps in ribosome recycling Peske et al. also showed that RRF and EF-G together with GTP promoted the dissociation of 50S subunits from the post-termination complex without involving translocation or a translocation-like event [12]. Another point of dispute is whether IF3 (initiation factor 3) is required for splitting of the post-termination ribosome in to subunits. Experiments from Ehrenberg and co-workers demonstrated that RRF and EF-G rapidly split the post-termination ribosome into subunits in the absence of IF3 by a mechanism that requires GTP, as well as GTP hydrolysis, and that the primary role of IF3 is to keep the subunits apart after the splitting event [7,13]. Recently, Peske et al. also indicated that IF3 did not affect subunit dissociation but prevented re-association, thereby masking the dissociation effect of EF-G and RRF under certain experimental conditions [12]. By contrast, Kaji and co-workers showed that 70 S ribosomes, as well as the model post-termination complexes, were dissociated into stable subunits by the co-operative action of three translation factors: RRF, EF-G and IF3 [14]. However, they also indicated that RRF and EF-G alone could transiently dissociate 70 S ribosomes, and that IF3 stabilized the dissociation by binding to the transiently formed 30 S subunits, preventing re-association back to 70 S ribosomes [14]. Thus the two statements about mechanisms of post-termination complex disassembly seem to resemble each other except in small details.

As major protein factors for disassembly of the post-termination complex, all reported RRFs are highly similar in amino acid sequence [15,16]. Crystal and solution structures of RRF have been solved from six different bacterial species [15–21]. All of these structures display a similar architecture and consist of two highly conserved domains: domain I displays a three-stranded α helix bundle structure, and domain II exists as a three layer $\beta/\alpha/\beta$

Abbreviations used: *aa*RRF, *Aquifex aeolicus* RRF; DTT, dithiothreitol; *Eco*DI/*Tte*DII, chimaera of *Eco*RRF domain I and *Tte*RRF domain II; EF-G, elongation factor-G; *Eco*EF-G, *Escherichia coli* EF-G; *Eco*RRF, *E. coli* RRF; GDPNP, guanidine 5′-(β,γ-imido)tri-phosphate; IF3, initiation factor 3; IPTG, isopropyl-β-D-thiogalactopyranoside; RF, release factor; RRF, ribosome recycling factor; *Tte*DI/*Eco*DII, chimaera of *Tte*RRF domain I and *Eco*RRF domain I; *Tte*EF-G, *Thermoanaerobacter tengcongensis* EF-G; *Tte*RRF, *T. tengcongensis* RRF; *Tth*EF-G, *Thermus thermophilus* EF-G; *Tth*RRF, *T. thermophilus* RRF.

[1] These authors contributed equally to this work.

[2] To whom correspondence should be addressed (email jinggzh@sun5.ibp.ac.cn).

Table 1 Strains and plasmids

Km^r, kanamycin resistant; Ap^r, ampicillin resistant; Cm^r, chloramphenicol resistant.

Strain	Characteristics	Source or reference
Bacteria		
T. tengcongensis	MB4^T A gram-negative anaerobic Eubacterium	[27]
E. coli		
LJ14	MC1061 *frr14*(ts)	[39]
DH5α	FΦ80d*lacZ*ΔM15 Δ(*lacZYA-argF*)*U169 deoR recA1 endA1 hsdR17*(rK$^-$mK$^+$) *phoA supE44*λ*.thi-1 gyra96relA1*	Nat. Lab. Biomacromolecules
BL21(DE3)pLysS	F$^-$ *ompT hadS*B(rB$^-$mB$^+$) *gal dcm* (DE3)/pLysS; Cm^r	Nat. Lab. Biomacromolecules
Plasmids		
pET-DB	T7 promoter-driven high-efficiency protein expression vector, encodes Km^r	[26]
pET-DB-*Tte*RRF	*T. tengcongensis* RRF gene cloned in to pET-DB, encodes Km^r	Present study
pET-28a(+)	T7 promoter-driven high-efficiency protein expression vector, encodes Km^r	Novagen
pET28-*Eco*RRF	*E. coli* RRF gene cloned in to pET-28a(+),encodes Km^r	Present study
pET28-*Eco*EF-G	*E. coli* EF-G gene cloned in to pET-28a(+),encodes Km^r	Present study
pET28-*Eco*DI/*Tte*DII	*Eco*DI/*Tte*DII cloned in to pET-28a(+),encodes Km^r	Present study
pET28-*Tte*DI/*Eco*DII	*Tte*DI/*Eco*DII cloned in to pET-28a(+),encodes Km^r	Present study
pET28-*Tte*EF-G	*T. tengcongensis* EF-G gene cloned in to pET-28a(+),encodes Km^r	Present study
pQE-60	T5 promoter/*lac* operator-driven protein expression vector, encodes Ap^r	Qiagen
pQE-*Eco*RRF	*E. coli* RRF gene cloned in to pQE-60, encodes Ap^r	Present study
pQE-*Tte*RRF	*T. tengcongensis* RRF gene cloned in to pQE-60, encodes Ap^r	Present study
pQE-*Eco*DI/*Tte*DII	*Eco*DI/*Tte*DII cloned in to pQE-60, encodes Ap^r	Present study
pQE-*Tte*DI/*Eco*DII	*Tte*DI/*Eco*DII cloned in to pQE-60, encodes Ap^r	Present study
pSTV28	Plasmid which is reconstructed from a replication start of pACYC184 and β-galactosidase gene including pUC118 multi-cloning site, encodes Cm^r	TaKaRa
pSTV28-*Tte*EF-G	*T. tengcongensis* EF-G gene cloned in to pSTV28, encodes Cm^r	Present study

sandwich structure. The two domains are arranged in an L-shaped conformation. Although the structure of RRF is well known, and disassembly of the post-termination complex by the concerted action of RRF and EF-G has been widely accepted, there still is not a full understanding of the RRF's structural features that are responsible for its mechanism of action. Recently, Rao and Varshney reported that although *Mycobacterium tuberculosis* RRF is non-functional in *Escherichia coli*, it regains activity upon the coexpression of *M. tuberculosis* EF-G [22]. Ito et al. also showed the same result when the function of *Thermus thermophilus* RRF was studied in *E. coli* [23]. These observations not only suggest the necessity for a specific interaction between the homologous RRF and EF-G in *E. coli* but also open a way to study interactions between the RRF and EF-G molecules. Three questions to be addressed are particularly interesting. Does each domain of RRF play a different role? If it does, which one is most responsible for the activity of disassembly of the post-termination complex? Is there any specific interaction between the domain II of RRF and EF-G? To answer these questions, two RRF chimaeras, *Eco*DI/*Tte*DII and *Tte*DI/*Eco*DII were created. *Eco*DI/*Tte*DII consists of domain I from *E. coli* RRF (*Eco*RRF) and domain II from *Thermoanaerobacter tengcongensis* RRF (*Tte*RRF) [24]. *Tte*DI/*Eco*DII consists of domain I from *T. tengcongensis* and domain II from *E. coli* RRF. The ribosome recycling activity of the RRF chimaeras was compared with wild-type RRFs using *in vivo* and *in vitro* activity assays. The experiments showed that like wild-type *Tte*RRF, the *Eco*DI/*Tte*DII chimaera failed to complement the RRF^{ts} (temperature sensitive) phenotype of the *E. coli* LJ14 (*frr*^{ts}) strain. However, under the same conditions, the *Tte*DI/*Eco*DII chimaera complemented the RRF^{ts} phenotype as efficiently as wild-type *Eco*RRF. It is noteworthy that although *Tte*RRF and *Eco*DI/*Tte*DII chimaeras are inactive in *E. coli* LJ14 (*frr*^{ts}), both of them regain activity upon coexpression of *T. tengcongensis* EF-G. These results indicate that domain II of RRF plays a crucial role in the function of RRF. The fact that *Tte*DI/*Eco*DII expressed with *Eco*EF-G, and *Eco*DI/*Tte*DII expressed with *Tte*EF-G, regain their activity in *E. coli* suggests that domain II of RRF is involved in a specific interaction between RRF and EF-G.

MATERIALS AND METHODS

Strains, plasmids, growth conditions and chemicals

The various bacterial strains and plasmids used in this study are listed in Table 1. Luria–Bertani broth [25] was used for bacterial growth. The media was supplemented with various antibiotics at the following final concentrations: ampicillin 50 μg/ml, kanamycin 50 μg/ml and chloramphenicol 25 μg/ml, as required. IPTG (isopropyl-β-D-thiogalactopyranoside) was added to a final concentration of 0.5 mM for RRF protein expression. For complementation of the *E. coli* RRF defect, various plasmids were transformed in to the *E. coli* LJ14 strain (*frr*^{ts}). Cultures were started with a 0.06 % (v/v) inoculum from freshly-grown (at 30 °C) overnight cultures, and growth at both permissive (30 °C) and non-permissive (42 °C) temperatures was monitored by recording culture turbidities at 600 nm at regular intervals. GDPNP [guanidine 5′-(β,γ-imido)tri-phosphate] (Sigma), a non-hydrolysable GTP analogue, was used for ribosome binding assays.

Cloning of the RRF gene from *T. tengcongensis*

The RRF gene from *T. tengcongensis* was cloned as described previously [24]. In brief, forward, 5′-GGTA**CCATGG**GTAG-CGATTATTTGAAAGACAGTG-3′ and reverse, 5′-GATT**GGA-TCC**TTAAATTTCCATTATCTCCTTTTC-3′ primers containing NcoI and BamHI restriction sites (bold) respectively, were designed to amplify the *T. tengcongensis* RRF gene by PCR using *T. tengcongensis* genomic DNA as the template DNA. The PCR product was inserted in to the NcoI and BamHI sites of pET-DB [26] after digestion with the same enzymes, resulting in pET-DB-*Tte*RRF for expression of *Tte*RRF. The RRF gene was also

cloned into the pQE-60 vector between the NcoI and BamHI sites, resulting in pQE-*Tte*RRF for the complementation assay.

Cloning of the EF-G gene from *T. tengcongensis*

Based on the putative EF-G gene sequence of *T. tengcongensis* [27] a forward, 5′-AGACAGC**CATATG**CCAAGGGATTTCAGCTTAGATAAAGTTAGG-3′ and a reverse, 5′-GCAA**GGATCC**TTATTTTTTTGCTGATAATATTTGCTCAGC-3′ primer containing NdeI and BamHI sites (bold) respectively, were designed to amplify the *T. tengcongensis* EF-G gene by PCR using *T. tengcongensis* genomic DNA as a template. The PCR product was inserted into the NdeI and BamHI sites of pET-28(+) after digestion with the same enzymes, resulting in pET-28-*Tte*EF-G for expression of *Tte*EF-G. The EF-G gene was also cloned into the pSTV-28 vector between the KpnI and BamHI sites, resulting in pSTV-*Tte*EF-G for the complementation assay.

Cloning of the RRF gene from *E. coli*

Forward, 5′-GGCA**CCATGG**GTATTAGCGATATCAGAAAAGATGC-3′ and reverse, 5′-GCTG**CTCGAG**GAACTGCATCAGTTCTGCTTCTTTG-3′ primers containing NcoI and XhoI restriction sites (bold), respectively, were used to amplify the *E. coli* RRF gene from *E. coli* genomic DNA [28]. The PCR product was digested with *NcoI* and *XhoI* and cloned into pET-28a(+) after digestion with the same enzymes, resulting in pET28-*Eco*RRF for expression of *Eco*RRF. The *Eco*RRF gene was also cloned into the pQE-60 vector between the NcoI and BamHI sites, resulting in pQE-*Eco*RRF for the complementation assay.

Cloning of the EF-G gene from *E. coli*

Based on the EF-G gene sequence of *E. coli* [29] forward, 5′-AGACAGCAGC**CATATG**GCTCGTACAACACCCATCGCACGCTACCG-3′ and reverse, 5′-GCAA**GGATCC**TTATTTACCACGGGCTTCAATTACGGCCTGAGCAACG-3′ primers containing NdeI and BamHI restriction sites (bold) respectively, were designed to amplify the *E. coli* EF-G gene by PCR using genomic DNA from *E. coli* DH5α as the template DNA. The PCR product was inserted into the NdeI and BamHI sites of pET-28(+) after digestion with the same enzymes, resulting in pET28-*Eco*EF-G for expression of *Eco*EF-G.

Cloning of chimaeric RRF variants

Two chimaeric RRF variants were constructed by using gene SOEing (gene splicing by overlap extension) [30]. For construction of the *Eco*DI/*Tte*DII chimaera gene, six primers were designed. Primers 1 and 2 were the same as the forward and reverse primers used for cloning of the RRF gene from *E. coli* as described above. The other four primers were as follows: primer 3, 5′-**AGGGCCGGATTCGCTCT**ACCCGTGCGTATTTTGCTG-3′; primer 4, 5′-**CAGCAAAATACGCACGGGT**AGAGCGAATCCGGCCCT-3′; primer 5, 5′-**GTTCTTCCGTCAGCGG**TGGAAGGACCAGTCTTAG-3′; primer 6, 5′-**CTAAGACTGGTCCTTCCA**CCGCTGACGGAAGAAC-3′. Each primer contained a priming sequence for the amplification of the *Eco*RRF gene or the *Tte*RRF gene and also has an overlapping sequence at its 5′ end (bold) that is complementary to a segment of the *Eco*RRF gene or the *Tte*RRF gene. Five PCRs were performed using the pQE-*Eco*RRF or pQE-*Tte*RRF plasmid as a template. The PCR product was digested with *NcoI* and *XhoI* and cloned into pET-28a(+) after digestion with the same enzymes, resulting in pET28-*Eco*DI/*Tte*DII for expression of *Eco*DI/*Tte*DII. The *Eco*DI/*Tte*DII gene was also cloned into the pQE-60 vector between the NcoI and BamHI sites, resulting in pQE-*Eco*DI/*Tte*DII, which was used for the complementation assay. The *Tte*DI/*Eco*DII chimaera gene was created by using the same strategy, resulting in pET28-*Tte*DI/*Eco*DII and pQE-*Tte*DI/*Eco*DII for expression of *Tte*DI/*Eco*DII and for the complementation assay respectively.

Purification of *Tte*RRF, *Eco*RRF, *Eco*DI/*Tte*DII, *Tte*DI/*Eco*DII, *Eco*EF-G and *Tte*EF-G

All proteins were expressed in a soluble form, details of the purification and characterization of the proteins were described previously [24]. In brief, each plasmid was transformed in to *E. coli* BL21 (DE3) pLysS cells respectively. Fresh cultures of transformants were induced with 0.5 mM IPTG, and the overexpressed proteins were purified by metal chelating affinity chromatography [24,31]. Each purified protein appeared as a single band on an SDS 15 % polyacrylamide gel. The protein concentration was determined as described [32].

In vitro assays for RRF activity

For the *in vitro* polysome-breakdown assay, the tetracycline-treated polysome fraction was prepared from *E. coli* strain MRE600 [33,34] and used for the post-termination complex-disassembly reaction by RRF, as described previously [35,36]. A reaction mixture [250 μl; containing 10 mM Tris/HCl (pH 7.4), 8.2 mM $MgSO_4$, 80 mM NH_4Cl, 1 mM DTT (dithiothreitol), 0.16 mM GTP, 0.01 mM puromycin, 125 units of ribonuclease inhibitor, 1.0 unit of A_{260} polysomes, 60 μg of EF-G, and 30 μg of RRF] was incubated at 30 °C for 20 min, and fractionated on 15–30 % sucrose density gradients by centrifugation at 190 000 ***g*** for 1 h. The gradients were scanned from top to bottom at 254 nm using a Hitachi gradient fraction collector.

Binding of RRF to 70 S ribosome in the presence or absence of EF-G

E. coli 70 S ribosome was prepared as described previously [34]. Complexes of EF-G and 70 S ribosome were prepared by mixing EF-G and ribosomes (molar ratio of EF-G/ribosome = 4) for 10 min at 30 °C before addition of RRF in an assay buffer with or without 3 μM GDPNP [10 mM Tris/HCl (pH 7.4), 8.2 mM $MgSO_4$, 80 mM NH_4Cl, 1 mM DTT and 50 μM puromycin]. Binding of RRFs to 70 S ribosome or the EF-G–ribosome complexes (with or without GDPNP) was measured using a filtering technique [16,37]. Briefly, various RRFs were incubated with 70 S ribosome or the complex (0.25 μM) in 40 μl of the assay buffer at 30 °C for 10 min. The mixture was applied on to Microcon YM-100 columns (Millipore) and centrifuged for 5 min at 3000 ***g*** to trap the ribosome-bound RRFs. Then 40 μl of the same buffer was loaded onto the column and centrifuged for 10 min at 3000 ***g*** to wash out the unbound RRFs. After two washes, the filter was incubated with 40 μl of the buffer for 1 min at room temperature. The ribosome-bound RRFs were collected from the inverted column by centrifugation. The recovered RRFs were detected by Western blotting with rabbit anti-(*E. coli* RRF) antibody (1:1000 dilution). Bound RRFs were quantified by the blotting of known amounts of RRF standards. To quantify non-specific binding between RRFs and the filter apparatus, control experiments without ribosomes were performed.

Release of RRFs from the RRF–ribosome complexes by EF-G

70 S ribosome (0.25 μM) and RRFs (4.0 μM) were incubated together for 10 min at 30 °C in 40 μl of assay buffer solution containing 0.5 mM GTP. Unbound RRFs were isolated by the Microcon YM-100 ultrafiltration method as described above. Various amounts of EF-Gs were added and incubated in the same buffer for 15 min at 30 °C. The mixture was subjected to Microcon

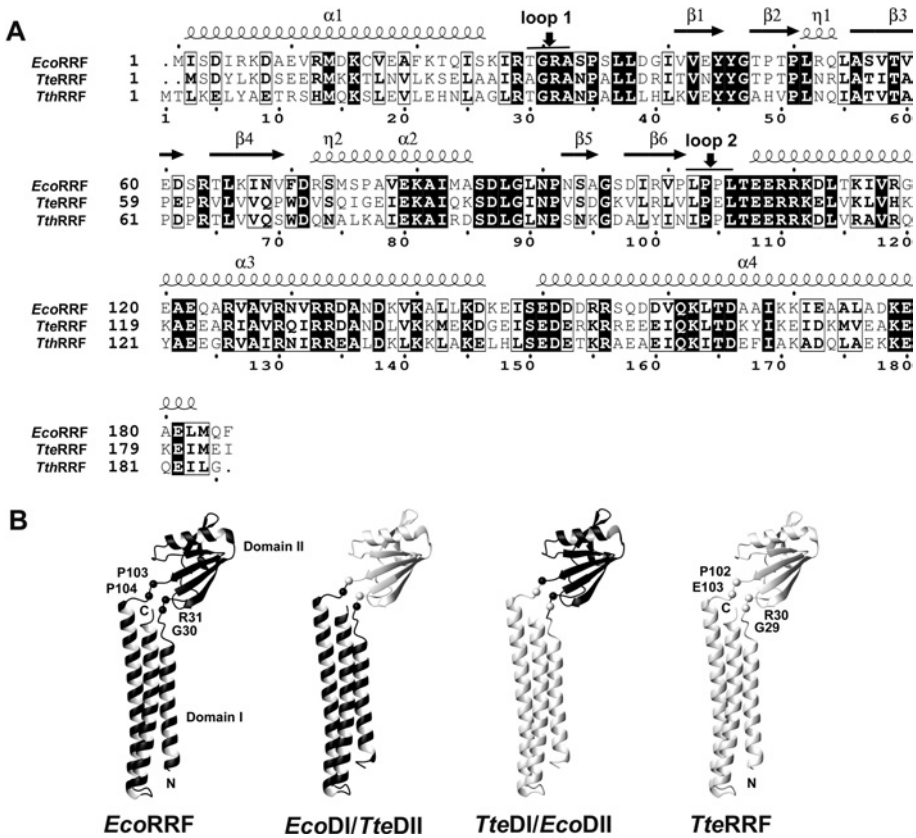

Figure 1 (A) Comparison of the primary structures of EcoRRF with TteRRF

Amino acid sequences are shown as single letter codes. The numbering at the bottom is the amino acid sequence from *T. thermophilus* RRF. Identical residues are shadowed in black and similar residues are boxed. The corresponding secondary-structure elements of *Eco*RRF are indicated at the top. Vertical arrows indicate the points where the two domains were exchanged (G30 and R31, P103 and P104 for *Eco*RRF; G29 and R30, P102 and E103 for *Tte*RRF respectively). (**B**) Schematic drawings of the structures of *Eco*RRF, *Tte*RRF, *Tte*DI/*Eco*DII, and *Eco*DI/*Tte*DII.

YM-100 ultrafiltration to separate ribosomes from the released RRFs. The remaining ribosome-bound RRF was determined via quantitative Western blotting [16,37].

RESULTS

Construction of chimaeric RRF variants

As described in the Materials and methods section, two RRF chimaeras were constructed. *Eco*DI/*Tte*DII consists of domain I from *E. coli* and domain II from *T. tengcongensis*, whereas *Tte*DI/*Eco*DII consists of domain I from *T. tengcongensis* and domain II from *E. coli*. As known, the RRFs from different bacteria are highly conserved in their primary structure and the three-dimensional structure of the RRFs from six bacterial organisms is also highly conserved [15–21], consisting of two domains. The two domains are connected to each other by two loops acting as a hinge region. Sequence alignment of *Tte*RRF and *Eco*RRF (Figure 1A) shows that loop 1 of the hinge is composed of T^{29}**GR**A^{32} for *Eco*RRF and A^{28}**GR**A^{31} for *Tte*RRF, loop 2 of the hinge is composed of L^{102}**PP**L^{105} for *Eco*RRF and L^{101}**PE**L^{104} for *Tte*RRF. The points where the domain swaps were chosen between **Gly–Arg** of loop 1, and **Pro–Pro** or **Pro–Glu** of loop 2 (Figure 1A) ensure that the domains of the RRF chimaeras retain their intact amino acid sequence. In order to clearly show the domain swaps between *Eco*RRF and *Tte*RRF, Figure 1(B) shows schematic drawings of the structures of *Eco*RRF, *Tte*RRF, *Tte*DI/*Eco*DII and *Eco*DI/*Tte*DII. It is noteworthy that our previous study showed that the secondary CD profiles of *Tte*RRF, *Eco*RRF, *Tte*DI/*Eco*DII and *Eco*DI/*Tte*DII are very similar [24]. This suggests that domain swaps between *Eco*RRF and *Tte*RRF have no significant effect on their folded structures.

*Tte*RRF alone does not rescue the temperature-sensitive phenotype of *E. coli* LJ14 (*frr*^{ts})

It is known that RRF is an essential protein for bacterial growth since deletion of the RRF gene is lethal in *E. coli* [38], as are temperature sensitive (*frr*^{ts}) mutations [39]. Complementation analysis allowed the *in vivo* activity of RRF to be tested. The *Tte*RRF gene cloned in pQE-*Tte*RRF was tested for intergeneric complementation of the *E. coli* LJ14 (*frr*^{ts}) strain. The growth rates of the various transformants in liquid cultures at the permissive (30 °C) and non-permissive (42 °C) temperatures were investigated. As shown in Figure 2(A), at the permissive temperature, transformants harbouring pQE-*Tte*RRF, pQE-*Eco*RRF, pQE-*Eco*DI/*Tte*DII or pQE-*Tte*DI/*Eco*DII grew at the same rate as those harbouring the vector pQE-60 alone, suggesting that the expression of these RRFs was not toxic to *E. coli*. However, at the non-permissive temperature, the transformants harbouring pQE-*Eco*RRF grew well, whereas those harbouring either the vector pQE-60 or pQE-*Tte*RRF did not. The growth of transformants harbouring pQE-*Tte*RRF was significantly delayed (Figure 2B). This observation indicates that *Tte*RRF alone does not rescue the temperature-sensitive phenotype of *E. coli* LJ14 (*frr*^{ts}). It is noteworthy that immuno-blot analysis of the cell-free extracts of *E. coli* LJ14 harbouring pQE-*Tte*RRF, pQE-*Eco*RRF, pQE-*Eco*DI/*Tte*DII, pQE-*Tte*DI/*Eco*DII or pQE-60 plasmids

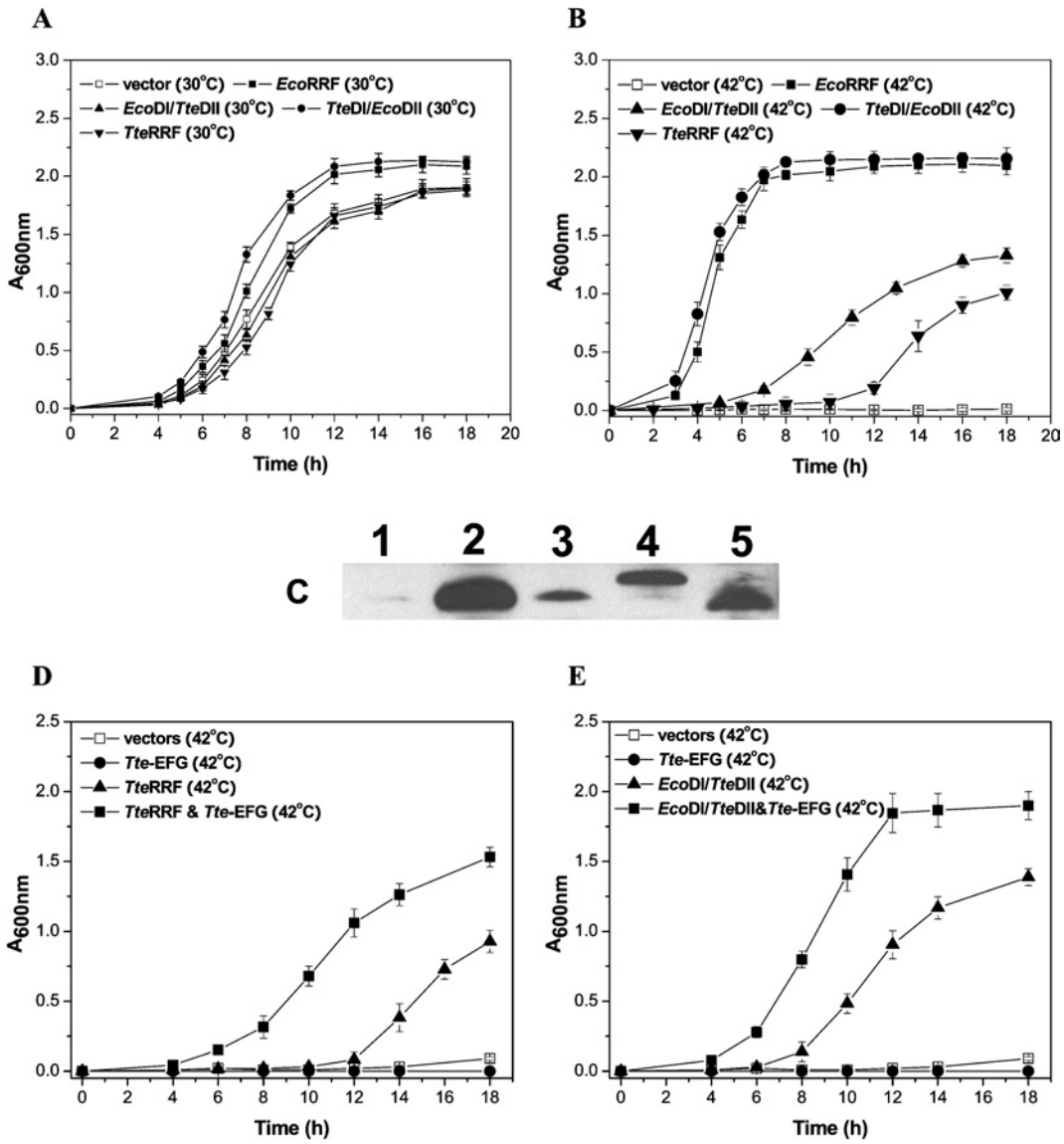

Figure 2 Complementation analysis of *E. coli* LJ14 with RRFs

The *E. coli* LJ14 (*frr*^{ts}) strain was transformed with the respective plasmids and examined for growth-phenotype. (**A**) Growth curves of various transformants of *E. coli* LJ14 (*frr*^{ts}) at the permissive temperature (30 °C). Vector, transformants with pQE-60; *Eco*RRF, transformants with pQE-*Eco*RRF; *Eco*DI/*Tte*DII, transformants with pQE-*Eco*DI/*Tte*DII; *Tte*DI/DII, transformants with pQE-*Tte*DI/*Eco*DII; *Tte*RRF, transformants with pQE-*Tte*RRF. (**B**) Growth curves of various transformants of *E. coli* LJ14 (*frr*^{ts}) at the non-permissive temperature (42 °C). The transformants are the same as those indicated in (**A**). (**C**) Detection of RRF expression in *E. coli* LJ14 by immunoblotting using anti-*Eco*RRF antibodies. Protein extracts were prepared from transformants harbouring the respective plasmids. Bands: 1, pQE-60 vector; 2, PQE-*Eco*RRF; 3, pQE-*Tte*RRF; 4, pQE-*Eco*DI/*Tte*DII; 5, pQE-*Tte*DI/*Eco*DII. (**D**) Growth curves of various transformants of *E. coli* LJ14 (*frr*^{ts}) at the non-permissive temperature (42 °C). Vectors, transformants with pQE-60 and pSTV-28; *Tte*EF-G, transformants with pQE-60 and pSTV-*Tte*EF-G; *Tte*RRF, transformants with pQE-*Tte*RRF and pSTV-28; *Tte*RRF and *Tte*-EFG, transformants with pQE-*Tte*RRF and pSTV-*Tte*EF-G. (**E**) Growth curves of various transformants of *E. coli* LJ14 (*frr*^{ts}) at the non-permissive temperature (42 °C). Vectors, transformants with pQE-60 and pSTV-28; *Tte*-EFG, transformants with pQE-60 and pSTV-*Tte*EF-G; *Eco*DI/*Tte*DII, transformants with pQE-*Eco*DI/*Tte*DII and pSTV-28; *Eco*DI/*Tte*DII&*Tte*-EFG, transformants with pQE-*Eco*DI/*Tte*DII and pSTV-*Tte*EF-G. The experimental conditions are described in the text.

respectively, grown at both the permissive (30 °C) and the non-permissive temperature (42 °C) showed that all the RRFs were expressed in the LJ14 strain (Figure 2C). This result ruled out the lack of *Tte*RRF expression as a possible reason for failure to rescue the RRF^{ts} phenotype of the LJ14 strain.

*Tte*DI/*Eco*DII RRF rescues the temperature-sensitive phenotype of *E. coli* LJ14 (*frr*^{ts})

*Tte*DI/*Eco*DII is a chimaeric RRF in which the domain I and II are from *T. tengcongensis* and *E. coli* respectively. Complementation analysis of *E. coli* LJ14 (*frr*^{ts}) strain with the *Tte*DI/*Eco*DII RRF gene, which was cloned into pQE-*Tte*DI/*Eco*DII, was performed. As shown in Figure 2(B), transformants harbouring pQE-*Eco*RRF or pQE-*Tte*DI/*Eco*DII grew at the same rate at the non-permissive temperature. This observation indicates that *Tte*DI/*Eco*DII RRF does rescue the temperature-sensitive phenotype of *E. coli* LJ14 (*frr*^{ts}) as efficiently as *Eco*RRF.

*Eco*DI/*Tte*DII RRF does not efficiently rescue the temperature-sensitive phenotype of *E. coli* LJ14 (*frr*^{ts})

*Eco*DI/*Tte*DII is another chimaeric RRF in which the domains I and II are from *E. coli* and *T. tengcongensis* respectively.

The *Eco*DI/*Tte*DII gene cloned into pQE-*Eco*DI/*Tte*DII was also tested for complementation of the *E. coli* LJ14 (*frr*^{ts}) strain. Figure 2(B) also showed the growth rate of transformants harbouring pQE-*Eco*DI/*Tte*DII at the non-permissive temperature. Compared with the growth rate of *E. coli* LJ14 harbouring pQE-*Eco*RRF and pQE-*Tte*DI/*Eco*DII at the non-permissive temperature, the growth rate of *E. coli* LJ14 harbouring pQE-*Eco*DII/*Tte*DII is much slower and is close to that of *Tte*RRF, indicating that like *Tte*RRF, *Eco*DI/*Tte*DII does not rescue the temperature-sensitive phenotype of *E. coli* LJ14.

Like *T. thermophilus* RRF [40], in spite of the apparent defect in complementation, slow growth of the transformants harbouring pQE-*Tte*RRF was observed after prolonged growth (Figure 2B), suggesting that weak residual activity may remain in *Tte*RRF in *E. coli*. It is noteworthy that compared with *Tte*RRF, the transformant harbouring pQE-*Eco*DI/*Tte*DII shows more activity for complementation of the *E. coli* LJ14 (*frr*^{ts}) strain (Figure 2B). This suggests that the interaction between domain I of *E. coli* RRF and domain II of *T. tengcongensis* RRF may allow *Eco*DI/*Tte*DII to gain some activity.

Both *Tte*RRF and *Eco*DI/*Tte*DII require *Tte*EF-G to rescue the temperature-sensitive phenotype of *E. coli* LJ14 (*frr*^{ts})

To examine whether *Tte*RRF or *Eco*DI/*Tte*DII regains activity upon coexpression of *Tte*EF-G in *E. coli*, the *E. coli* strain LJ14 (*frr*^{ts}) harbouring pQE-*Tte*RRF or pQE-*Eco*DI/*Tte*DII was transformed with pSTV-*Tte*EF-G expressing *Tte*EF-G, and the growth of transformants was monitored at the non-permissive temperature (42 °C). As shown in Figures 2(D) and 2(E), the growth rate of transformants harbouring pQE-*Tte*RRF and pSTV-*Tte*EF-G, or pQE-*Eco*DI/*Tte*DII and pSTV-*Tte*EF-G was significantly improved, compared with that of transformants harbouring pQE-*Tte*RRF or pQE-*Eco*DI/*Tte*DII alone. These observations indicate that both *Tte*RRF and *Eco*DI/*Tte*DII can rescue the temperature-sensitive phenotype of *E. coli* LJ14 (*frr*^{ts}) upon coexpression of *Tte*EF-G.

It can be seen that compared with the *Tte*RRF (Figure 2D), the transformant harbouring pQE-*Eco*DI/*Tte*DII also shows more activity for complementation of the *E. coli* LJ14 (*frr*^{ts}) strain (Figure 2E), even upon coexpression of *Tte*EF-G. Thermostability of *Tte*RRF, *Eco*RRF and *Eco*DI/*Tte*DII was studied by using heat induced denaturation. The thermostability of *Eco*DI/*Tte*DII is close to *Eco*RRF, whereas *Tte*RRF is still stable at above 85 °C [24]. This observation suggests that *Eco*DI/*Tte*DII should have more flexibility than *Tte*RRF for its functional expression in *E. coli* at 42 °C. This may be another reason why the transformant harbouring pQE-*Eco*DI/*Tte*DII always shows more activity on complementation of the *E. coli* LJ14 (*frr*^{ts}) strain than that harbouring *Tte*RRF (Figures 2B, 2D and 2E).

Polysome-breakdown activity of wild-type RRFs and their chimaeric RRFs

To further confirm ribosome recycling activities of wild-type RRFs and their chimaeric RRFs, *in vitro* polysome breakdown assays were performed using factor-free polysomes prepared from *E. coli* MRE600 according to the method described by Kaji and co-workers [35,36]. As shown in Figure 3(B), *Eco*RRF and *Tte*DI/*Eco*DII RRF show polysome-breakdown activity in the present assay system containing *E. coli* polysomes and *Eco*EF-G. By contrast, *Tte*RRF and *Eco*DI/*Tte*DII RRF do not show any polysome-breakdown activity under the same conditions. However, when *Eco*EF-G was replaced with *Tte*EF-G in the assay system, all four RRFs showed some polysome-breakdown activity [Figure 3B, right column compare with Figure 3A (polysomes alone)]. However, *Tte*RRF, and especially *Eco*DI/*Tte*DII showed more polysome-breakdown activity.

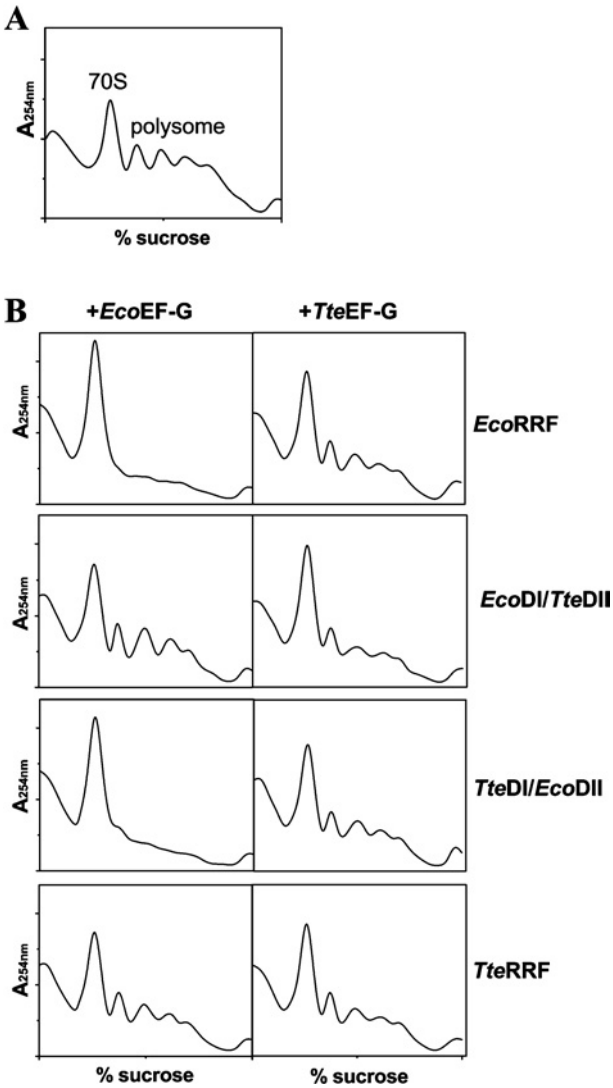

Figure 3 Polysome-breakdown assays of RRFs

Reactions were set up as described in the Materials and methods section. (**A**) Polysomes alone; (**B**) left column, RRFs with *Eco*EF-G; right column, RRFs with *Tte*EF-G. Each reaction mixture contains 30 μg of RRF and 60 μg of *Eco*EF-G or *Tte*EF-G.

Release of RRF by EF-G from *E. coli* 70 S ribosomes was also performed. Complexes of 70 S ribosomes and RRFs were prepared as described in the Materials and methods section. As shown in Figure 4(A), *Eco*EF-G releases *Eco*RRF and *Tte*DI/*Eco*DII from ribosomes in a dose-dependent manner, but does not release *Tte*RRF and *Eco*DI/*Tte*DII from ribosomes. By contrast, *Tte*EF-G has more activity for the release of *Tte*RRF, especially for the release of *Eco*DI/*Tte*DII from ribosomes (Figure 4B). These results correspond well with the above *in vitro* polysome-breakdown activity of wild-type RRFs and their chimaeric RRFs, suggesting a specific interaction between RRF and EF-G.

Binding of wild-type RRFs and their chimaeric RRFs to ribosomes

To test whether different RRFs have different binding capacities for the *E. coli* ribosome and whether the lack of activity of *Tte*RRF and *Eco*DI/*Tte*DII in *E. coli* polysome breakdown is due to the loss of binding capacity to the *E. coli* ribosome, the ability of *Eco*RRF,

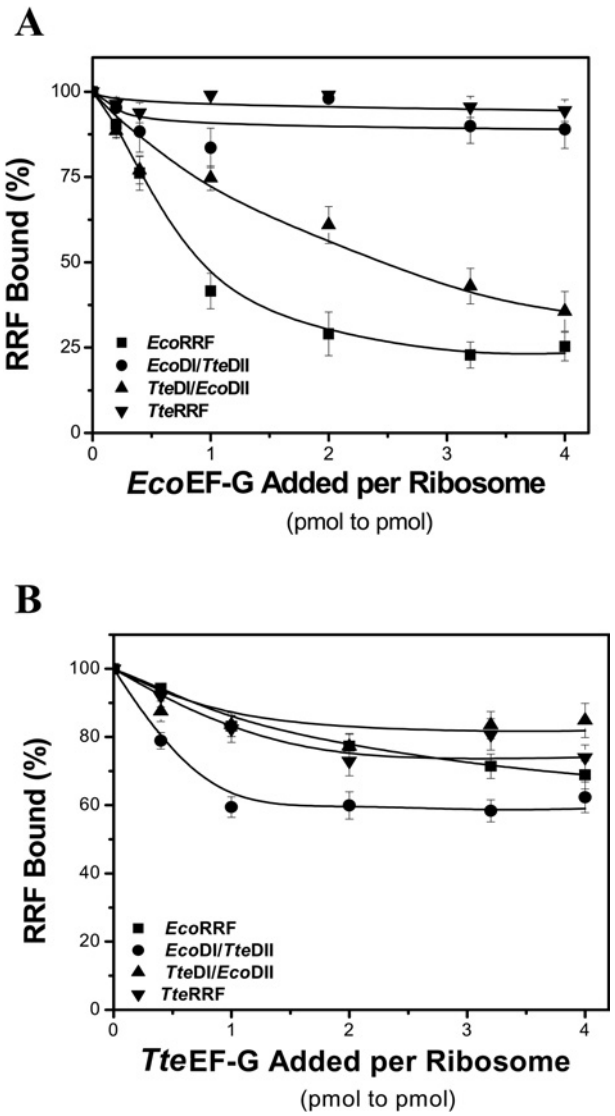

Figure 4 EF-Gs release RRFs from 70 S ribosomes in a dose-dependent manner

Complexes of *Eco*RRF, *Eco*DI/*Tte*DII, *Tte*DI/*Eco*DII or *Tte*RRF (4 μM) with 70 S ribosomes (0.25 μM) were formed in 40 μl of assay buffer solution as described in the Material and methods section. (**A**) Various amounts of *Eco*EF-G (0.05, 0.125, 0.25, 0.5, 0.75 and 1.0 μM) and GTP (0.5 mM) were then added and incubated at room temperature for 15 min. The mixture was subjected to Microcon-100 ultrafiltration to separate the ribosomes from the released RRFs. The remaining ribosome-bound RRFs were determined by quantitative Western blotting. The RRFs bound to ribosomes in the absence of EF-Gs was taken as 100 %. (**B**) Various amounts of *Tte*EF-G (0.05, 0.125, 0.25, 0.5, 0.75 and 1.0 μM) and GTP (0.5 mM) were applied to the assay system. Others are the same as in (**A**).

*Tte*RRF, *Eco*DI/*Tte*DII and *Tte*DI/*Eco*DII to bind to the *E. coli* 70 S ribosome was tested under different conditions as described in Materials and methods. Approximate dissociation constant (K_d) values were revealed from the dose-response curves according to the amounts of bound RRF determined by quantitative Western blotting (Figure 5). Although these measured K_d values may be overestimated because the filter technique is a non-equilibrium technique, these values should be relatively meaningful, as discussed by Hirokawa et al. [37]. Figure 5(A) shows the dose-response curves for binding of various amounts of RRFs to ribosomes in the absence of EF-G and GDPNP. The apparent K_d values of *Eco*RRF, *Eco*DI/*Tte*DII, *Tte*RRF, and *Tte*DI/*Eco*DII release from the 70 S ribosome were estimated to be in the range (1.0–2.4) $\times 10^{-6}$ M (Table 2). The apparent K_d values for all four RRFs in the presence of *Eco*EF-G are in the range of (0.20–0.25) $\times 10^{-6}$ M (Table 2), which are slightly lower than in the presence of *Tte*EF-G, (0.31–0.64) $\times 10^{-6}$ M (Table 2). Compared with the apparent K_d values in the absence of EF-G, this observation suggests that binding of EF-G to 70 S ribosome could facilitate RRF binding. However, in the presence of *Eco*EF-G and GDPNP, the apparent K_d values for all four RRFs are in the range (1.49–1.79) $\times 10^{-6}$ M (Table 2), which are slightly higher than that in the presence of *Tte*EF-G and GDPNP [(0.73–1.36) $\times 10^{-6}$ M, Table 2]. Compared with the apparent K_d values in the absence of GDPNP, the data presented above suggest the presence of EF-G–GDPNP slows down the binding of RRF to the 70 S ribosome. This result is consistent with the previous finding that EF-G in the GTP form, and RRF bind with negative co-operativity to the 70 S ribosome [11,13].

It is noteworthy that when the apparent dissociation constants obtained under the same conditions for all four RRFs were compared, the K_d values are of the same order of magnitude. This similarity of K_d values for all four RRFs suggests that: (i) all four RRFs have the same binding capacity to the 70 S ribosome; (ii) *Tte*RRF and *Eco*DI/*Tte*DII are non-functional in *E. coli* which is not due to the loss of their binding capacity to the *E. coli* ribosomes.

DISCUSSION

Role of RRF domain II and its implications for disassembly of the post-termination ribosome complex

Although disassembly of the post-termination complex by the concerted action of RRF and EF-G has been widely accepted, how RRF interacts with EF-G and disassembles the post-termination complex is not fully known. Many details of the sequential events responsible for the disassembly of the post-termination complex remain to be established. Functional studies utilizing heterologous RRF proteins in *E. coli* have made significant contributions towards understanding the structure-function relationship of this protein [15,22,23,40]. With genetic approaches, Nakamura and colleagues studied the viability of *E. coli* temperature-sensitive-lethal strains expressing heterologous RRF (*T. thermophilus* RRF) and wild-type or chimaeric EF-G variants. They identified a large number of mutations in both EF-G and RRF that could restore the recycling function of heterologous RRF in *E. coli* [10,23]. These findings not only confirm the necessity for a specific interaction between homologous EF-G and RRF as pointed out by Rao and Varshney [22], but also indicate that direct interaction between RRF and domain IV of EF-G is a prerequisite for ribosome disassembly. It is understandable from the view point of bio-evolution that a specific interaction between homologous EF-G and RRF is more favourable for their functional expression. However, Nakamura and colleagues demonstrated that *Aquifex aeolicus* RRF (*aa*RRF) shows a unique feature in heterologous expression and complementation in *E. coli* compared with other heterologous RRFs from *M. tuberculosis* [22] and *T. thermophilus* [23]. Like the latter two RRFs, *aa*RRF is non-functional in *E. coli*, but it remains inactive even in the presence of homologous *A. aeolicus* EF-G [41]. A chimaeric EF-G; however, composed of *E. coli* domains I–III and *A. aeolicus* domains IV–V in EF-G, was able to activate *aa*RRF in *E. coli*. Considering that domain IV of EF-G serves as a site for contact with RRF [23], and domain V is known to interact with the ribosome and to be essential for the positioning of domain IV [42], and domains I–III serve as contact sites with the ribosome [43], this finding might suggest that *aa*RRF is

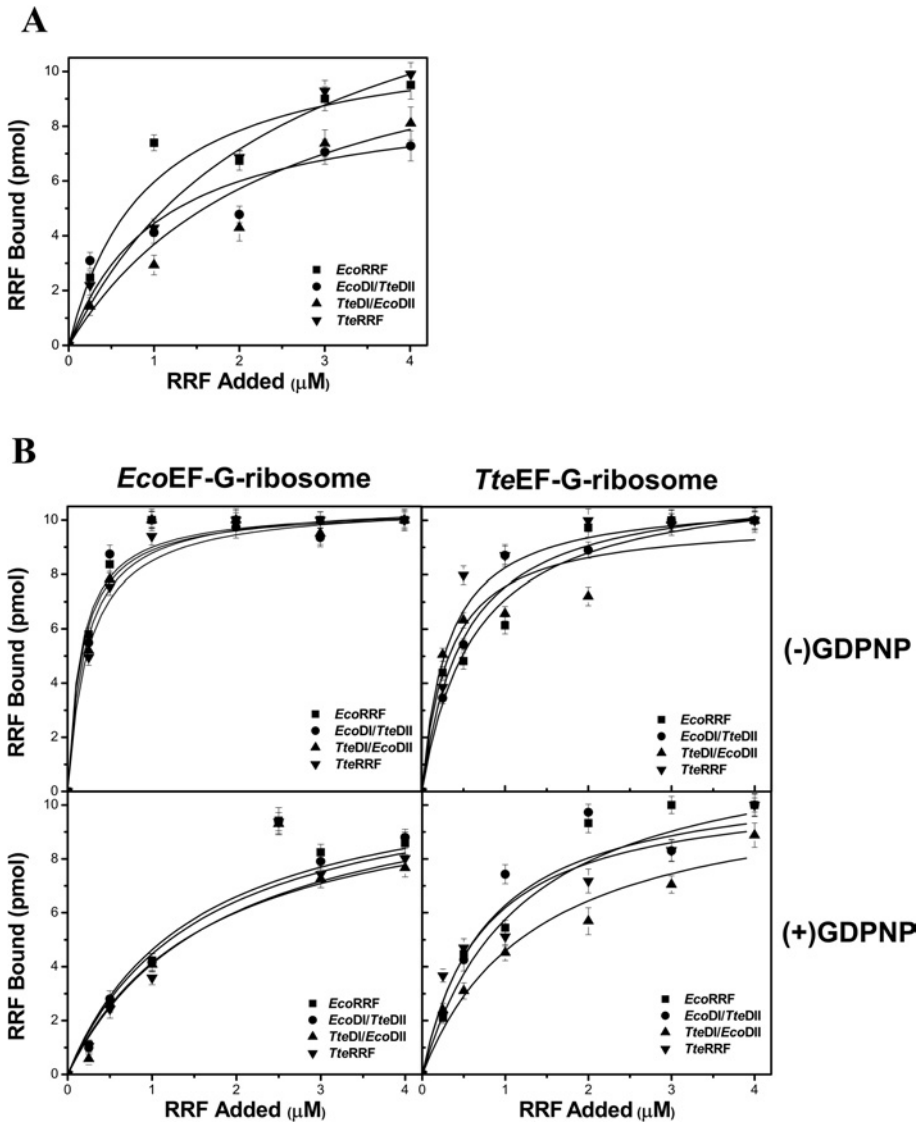

Figure 5 Binding of RRFs to 70 S *E. coli* ribosomes under different conditions

(**A**) The dose-response curve for binding of various amounts of *Eco*RRF, *Eco*DI/*Tte*DII, *Tte*DI/*Eco*DII or *Tte*RRF to ribosomes in the absence of EF-Gs and GDPNP. The concentration of 70 S ribosomes is 0.25 μM. The RRF concentrations were from 0–4 μM. (**B**) The left column shows the binding curve of *Eco*RRF, *Eco*DI/*Tte*DII, *Tte*DI/*Eco*DII or *Tte*RRF to *Eco*EF-G–ribosome complexes without (top) or with (bottom) 3.0 μM GDPNP; the right column shows the binding curve of *Eco*RRF, *Eco*DI/*Tte*DII, *Tte*DI/*Eco*DII or *Tte*RRF to *Tte*EF-G–ribosome complexes without (top) or with (bottom) 3.0 μM GDPNP. The concentrations of *Eco*EF-G and *Tte*EF-G were 1 μM respectively. Other conditions were similar to those in (**A**).

Table 2 The apparent K_d values of *Eco*RRF, *Eco*DI/*Tte*DII, *Tte*RRF and *Tte*DI/*Eco*DII from the 70 S ribosome under different conditions

	K_d ($\times 10^{-6}$ M)				
	EF-G (−)	*Eco*EF-G (+)		*Tte*EF-G (+)	
RRF	GDPNP (−)	GDPNP (−)	GDPNP (+)	GDPNP (−)	GDPNP (+)
*Eco*RRF	0.92 ± 0.26	0.18 ± 0.04	1.55 ± 0.40	0.64 ± 0.20	1.19 ± 0.29
*Eco*DI/*Tte*DII	1.06 ± 0.31	0.16 ± 0.06	1.49 ± 0.39	0.50 ± 0.10	0.78 ± 0.32
*Tte*DI/*Eco*DII	2.45 ± 0.73	0.21 ± 0.06	1.65 ± 0.68	0.32 ± 0.12	1.36 ± 0.50
*Tte*RRF	2.48 ± 0.42	0.25 ± 0.04	1.79 ± 0.72	0.31 ± 0.10	0.73 ± 0.18

defective in its functional co-ordination with domain IV of *Eco*EF-G whereas *A. aeolicus* EF-G domains I–III are defective in their functional co-ordination with the ribosome. The above results further suggest that two key processes are required in functional post-termination ribosome recycling: interaction of *aa*RRF with EF-G through domain IV and the functional co-ordination with the ribosome through EF-G domains I–III. Hence the chimaeric EF-G, *Eco*I–III/*aa*IV–V, resolves both problems. Of course, this result suggests that in addition to EF-G domain IV, which serves as the site of contact with RRF [23], the interaction of EF-G

domains I–III with the ribosome also plays a pivotal role in post-termination ribosome disassembly.

The above results demonstrate that clarification of the function of the individual domains of EF-G is very important for fully understanding the mechanism of the post-termination ribosome complex disassembly. In this report, to clarify the function of the individual domains of RRF, two RRF chimaeras, *Eco*DI/*Tte*DII and *Tte*DI/*Eco*DII, were created by domain swaps between the *E. coli* and *T. tengcongensis* RRF proteins. The ribosome recycling activity of the RRF chimaeras was compared with wild-type RRFs using *in vivo* and *in vitro* activity assays. *Tte*RRF and *Eco*DI/*Tte*DII are non-functional in *E. coli* as compared with *Eco*RRF (Figures 2B and 3B). To test whether the lack of activity of *Tte*RRF and *Eco*DI/*Tte*DII in *E. coli* is due to the loss of binding capacity to the *E. coli* ribosome, we tested the binding ability of *Eco*RRF, *Tte*RRF, *Eco*DI/*Tte*DII and *Tte*DI/*Eco*DII to the *E. coli* ribosome. The latter three RRFs bind *in vitro* to the *E. coli* 70 S ribosome as efficiently as *Eco*RRF (Figure 5). This observation suggests that *Tte*RRF and *Eco*DI/*Tte*DII do not interact properly with the *E. coli* EF-G. Interestingly, like *Eco*RRF, *Tte*DI/*Eco*DII is fully functional in *E. coli* (Figures 2B and 3B), suggesting that *Tte*DI/*Eco*DII interacts with the *E. coli* EF-G as efficiently as *Eco*RRF, and the domain II of *E. coli* RRF directly interacts with the *E. coli* EF-G. To validate this scenario, we further tested whether *Tte*RRF and *Eco*DI/*Tte*DII could be activated by coexpression of their homologous EF-G (*Tte*EF-G) in *E. coli*. As expected, both *Tte*RRF and *Eco*DI/*Tte*DII can be activated by coexpression of *Tte*EF-G in *E. coli*. The ability of *Tte*EF-G to activate both *Tte*RRF and *Eco*DI/*Tte*DII in *E. coli* further confirms the necessity for a specific interaction between the domain II of *Tte*RRF and the *Tte*EF-G. This is consistent with the structural model for RRF action on the 70 S ribosome, provided by Wilson et al. [44], in which domain II of RRF makes contact with domain IV of EF-G, whereas the hinge region of RRF nestles against domain III of EF-G. While preparing this manuscript, we became aware of a recent study on the mechanisms for the disassembly of the post-termination complex inferred from cryo-electron microscopy studies [45]. Using this technique, Gao et al. obtained two density maps: one of the RRF bound post-termination complex and one of the 50 S subunit bound with both EF-G and RRF. Comparing the two maps, Gao et al. found domain I of RRF to be in the same orientation, while domain II in the EF-G-containing 50 S subunit is extensively rotated (approx. 60°) compared with its orientation in the 70 S complex. The rotation is induced by the presence of EF-G, since domain I of RRF is firmly anchored in a pocket of rRNA helices. Mapping the 50 S conformation of RRF on to the 70 S post-termination complex suggests that the domain II movement can disrupt the intersubunit bridges B2a and B3, and could therefore be the first step in ribosome splitting into subunits [44]. Taking these results into consideration, it could be concluded that domain II of RRF plays a crucial role in the concerted action of RRF and EF-G for the post-termination complex disassembly.

Domain I of the RRF molecule mainly contributes to ribosome binding

To elucidate how the RRF molecule interacts with the ribosome and which part of the RRF molecule is mainly responsible for binding to the ribosome is important for fully understanding the mechanism of post-termination ribosome disassembly. Interaction of RRF with *E. coli* ribosomes, first studied by the surface plasmon resonance technique, showed that RRF interacts with 70 S ribosomes as well as 50 S and 30 S subunits, but RRF interacts preferentially with 50 S subunits [46]. Then binding of *Vibrio parahaemolyticus* RRF and its domain I (RRF-DI) to *E. coli* 70 S ribosome or its subunits was measured by a filtering technique, in which non-specific binding of wild-type RRF and RRF-DI to filter apparatus was found to be negligible [16]. This experiment showed that both wild-type RRF and RRF-DI of *V. parahaemolyticus* are bound to the 70 S ribosome and the 50 S subunit but not to the 30 S subunit. Polysome-breakdown assay of RRF-DI showed that RRF-DI does not show any ribosome recycling activity, but it inhibits wild-type RRF activity. These results suggest that both RRF-DI and wild-type RRF share the same binding site [16]. It can be inferred that the reason for RRF-DI inhibition of its wild-type RRF activity is due to competition at the binding-site. Since the affinity of RRF-DI to 50 S subunits is equivalent to that of wild-type RRF, binding between RRF and the ribosome depends on the interaction between domain I of RRF and the 50 S subunit [16]. A recent study further showed that amino acid residues Glu^{122}–Arg^{133} and Gln^{161}–Asp^{165} within *E. coli* RRF domain I appear to form the most stable connection with 23 S rRNA [9], which corresponds well with the previous observation that R132H and R132G mutants were structurally similar to wild-type RRF but are non-functional, they failed to bind to 50 S subunits or 70 S ribosome [46]. Taking all the observations into consideration, it can be concluded that domain I of the RRF molecule mainly contributes to ribosome binding.

However, all the above observations were made *in vitro*. Further clarification was sought through the *in vivo* experiments carried out in this study. Since binding of RRF to ribosomes is a prerequisite for its function, comparison of the ribosome recycling activity of *Eco*RRF, *Tte*DI/*Eco*DII, *Tte*RRF and *Eco*DI/*Tte*DII *in vivo* provides useful evidence for the ribosome binding mechanism of the RRF molecule. As shown above, *Tte*DI/*Eco*DII and *Eco*RRF have the same ribosome recycling activity *in vivo*, as do *Eco*DI/*Tte*DII and *Tte*RRF (Figure 2), suggesting that both *Tte*RRF domain I (*Tte*DI) and *Eco*RRF domain I (*Eco*DI) should have the same binding affinity for the *E. coli* ribosome. The *in vitro* ribosome binding assays also show that all four RRFs can bind *E. coli* 70 S ribosome with almost the same apparent K_d values under the same conditions. Taken together, we could suggest that there is apparently not any species-specific binding to *E.coli* ribosomes for *Eco*RRF or *Tte*RRF. This notion is further supported by the latest works from Yamami et al. [41] and Gao et al. [45]. Yamami et al. showed that although *A. aeolicus* RRF is non-functional in *E. coli* and it remains inactive even upon coexpression of *A. aeolicus* EF-G, *A. aeolicus* RRF binds *in vitro* to *E. coli* ribosomes as efficiently as *Eco*RRF. As described above, Gao et al. showed domain I of RRF to be in the same orientation when bound to either the post-termination complex or the 50 S subunit, it is very tightly anchored in a pocket formed by several 23 S rRNA helices (His^{69}, His^{71}, His^{80}, His^{89}, His^{92} and His^{93}) of the peptidyl transfer centre. This observation is consistent with the fact that most of the conserved residues among the helix bundle are basic amino acids [15]. The positively charged armpit region may facilitate 'functional' loading of RRF on to the ribosome, in relation to EF-G, by electrostatic interaction with the negatively charged phosphate group of rRNA.

It is noteworthy that to highlight the major function of the individual domains of RRF does not mean that the other function of each domain is ruled out. The RRF molecule as a whole is involved in proper interactions with EF-G and ribosomes for the post-termination ribosome disassembly. Two key processes are required for post-termination ribosome recycling to become functional: interaction of RRF with EF-G through domain IV and the functional co-ordination with the ribosome through EF-G domains I-III. *Tte*RRF and *Eco*DI/*Tte*DII are non-functional

in *E. coli*, but they can be activated by coexpression of *Tte*EF-G in *E. coli*. This observation suggests that both *Tte*RRF and *Eco*DI/*Tte*DII interact incorrectly with *E. coli* EF-G. To find the structural basis for the interaction between *Tte*RRF and *Eco*EF-G or *Tte*EF-G, the structural features of *Tte*RRF were compared with its highly similar proteins, *Eco*RRF and *Tth*RRF from *E. coli* and *T. thermophilus* respectively. Figure 1(A) shows the primary and secondary structures of RRFs. The deduced amino acid sequence of *Tte*RRF shows a 51.4 % identity and 68.1 % similarity with that of *Eco*RRF, and a 50.5 % identity and 66.7 % similarity with that of *Tth*RRF. More importantly, the conserved or conservatively substituted residues on the molecular surface and in hydrophobic core residues are very similar to each other [15]. The structural similarity suggests that *Tte*RRF folds with a similar topology to other RRFs. However, amino acid sequence diversity between *Tte*RRF and *Eco*RRF is also observed. According to the docking simulation results of the 50 S–EF-G–GDPNP–RRF complex [45], *Eco*RRF residues $A^{94}GSD^{97}$ in β-sheet 5 of RRF domain II may interact with a fragment, E^{559}QLKAGPLAGY^{569}, in domain IV of *Eco*EF-G. However, the equivalent residues for *Tte*RRF, $D^{93}GKV^{96}$, are significantly different from those of *Eco*RRF. Moreover, the equivalent fragment, E^{546}AMQNGVLGGY^{556} in domain IV of *Tte*EF-G is also different from that in *Eco*EF-G. Interestingly, the equivalent amino acid sequences for both *Tth*RRF and *Tth*EF-G are similar to those in *Tte*RRF and *Tte*EF-G respectively. The difference in amino acid residues suggests that proper interactions between RRF and EF-G at their interfaces are essential for ribosome recycling. This may be one of the reasons why *Tte*RRF and *Eco*DI/*Tte*DII alone are nonfunctional in *E. coli*.

We thank Professor A. Kaji, Department of Microbiology, School of Medicine, University of Pennsylvania, PA, U.S.A. for providing *E. coli* LJ14 and MRE600 strains. We thank Dr S. Perrett (Institute of Biophysics, China) for critical reading of the manuscript and for valuable comments. We are also grateful to Z. N. Zhou and M. R. Zhang (Institute of Biophysics, China) for technical assistance. This work was supported by grants (G1999075608 and 3017021) from the China Committee for Science and Technology.

REFERENCES

1 Freistroffer, D. V., Pavlov, M. Y., MacDougall, J., Buckingham, R. H. and Ehrenberg, M. (1997) Release factor RF3 in *E. coli* accelerates the dissociation of release factors RF1 and RF2 from the ribosome in a GTP-dependent manner. EMBO J. **16**, 4126–4133
2 Zavialov, A. V., Buckingham, R. H. and Ehrenberg, M. (2001) A posttermination ribosomal complex is the guanine nucleotide exchange factor for peptide release factor RF3. Cell **107**, 115–124
3 Zavialov, A. V., Mora, L., Buckingham, R. H. and Ehrenberg, M. (2002) Release of peptide promoted by the GGQ motif of class 1 release factors regulates the GTPase activity of RF3. Mol. Cell **10**, 789–798
4 Janosi, L., Hara, H., Zhang, S. and Kaji, A. (1996) Ribosome recycling by ribosome recycling factor (RRF)- an important but overlooked step of protein synthesis. Adv. Biophys. **32**, 121–201
5 Janosi, L., Ricker, R. and Kaji, A. (1996) Dual functions of ribosome recycling factor in protein biosynthesis: disassembling the termination complex and preventing translational errors. Biochimie **78**, 959–969
6 Pavlov, M. Y., Freistroffer, D., MacDougall, J., Buckingham, R. H. and Ehrenberg, M. (1997) Fast recycling of *Escherichia coli* ribosomes requires both ribosome recycling factor (RRF) and release factor RF3. EMBO J. **16**, 4134–4141
7 Karimi, R., Pavlov, M. Y., Buckingham, R. H. and Ehrenberg, M. (1999) Novel roles for classical factors at the interface between translation termination and initiation. Mol. Cell **3**, 601–609
8 Lancaster, L., Kiel, M. C., Kaji, A. and Noller, H. F. (2002) Orientation of ribosome recycling factor in the ribosome from directed hydroxyl radical probing. Cell **111**, 129–140
9 Agrawal, R. K., Sharma, M. R., Kiel, M. C., Hirokawa, G., Booth, T. M., Spahn, C. M. et al. (2004) Visualization of ribosome-recycling factor on the *Escherichia coli* 70 S ribosome: function implications. Proc. Natl. Acad. Sci. U.S.A. **101**, 8900–8905
10 Fujiwara, T., Ito, K., Yamami, T. and Nakamura, Y. (2004) Ribosome recycling factor disassembles the posttermination ribosomal complex independent of the ribosomal translocase activity of elongation factor G. Mol. Microbiol. **53**, 517–528
11 Kiel, M. C., Raj, V. S., Kaji, H. and Kaji, A. (2003) Release of ribosome-bound ribosome recycling factor by elongation factor G. J. Biol. Chem. **278**, 48041–48050
12 Peske, F., Rodnina, M. V. and Wintermeyer, W. (2005) Sequence of steps in ribosome recycling as defined by kinetic analysis. Mol. Cell **18**, 403–412
13 Zavialov, A. V., Hauryliuk, V. V. and Ehrenberg, M. (2005) Splitting of the posttermination ribosome into subunits by the concerted action of RRF and EF-G. Mol. Cell **18**, 675–686
14 Hirokawa, G., Nijman, R. M., Raj, V. S., Kaji, H., Igarashi, K. and Kaji, A. (2005) The role of ribosome recycling factor in dissociation of 70 S ribosomes into subunits. RNA **11**, 1317–1328
15 Toyoda, T., Tin, O. F., Ito, K., Fujiwara, T., Kumasaka, T., Yamamoto, M., Garber, M. B. and Nakamura, Y. (2000) Crystal structure combined with genetic analysis of the *Thermus thermophilus* ribosome recycling factor shows that a flexible hinge may act as a functional switch. RNA **6**, 1432–1444
16 Nakano, H., Yoshida, T., Uchiyama, S., Kawachi, M., Matsuo, H., Kato, T., Ohshima, A., Yamaichi, Y., Honda, T., Kato, H. et al. (2003) Structure and binding mode of a ribosome recycling factor (RRF) from mesophilic bacterium. J. Biol. Chem. **278**, 3427–3436
17 Selmer, M., Al-Karadaghi, S., Hirokawa, G., Kaji, A. and Liljas, A. (1999) Crystal structure of *Thermotoga maritima* ribosome recycling factor: a tRNA mimic. Science (Washington D.C.) **286**, 2349–2352
18 Kim, K. K., Min, K. and Suh, S. W. (2000) Crystal structure of the ribosome recycling factor from *Escherichia coli*. EMBO J. **19**, 2362–2370
19 Nakano, H., Uchiyama, S., Yoshida, T., Ohkubo, T., Kato, H., Yamagata, Y. and Kobayashi, Y. (2002) Crystallization and preliminary X-ray crystallographic studies of a mutant of ribosome recycling factor from Escherichia coli, Arg132Gly. Acta Crystallogr. D Biol. **58**, 124–126
20 Yoshida, T., Uchiyama, S., Nakano, H., Kashimori, H., Kijima, H., Ohshima, T., Saihara, Y., Ishino, T., Shimahara, H., Yoshida, T. et al. (2001) Solution structure of the ribosome recycling factor from *Aquifex aeolicus*. Biochemistry **40**, 2387–2396
21 Saikrishnan, K., Kalapala, S. K., Varshney, U. and Vijayan, M. (2005) X-ray structural studies of *Mycobacterium tuberculosis* RRF and a comparative study of RRFs of known structure. Molecular plasticity and biological implications. J. Mol. Biol. **345**, 29–38
22 Rao, A. R. and Varshney, U. (2001) Specific interaction between the ribosome recycling factor and the elongation factor G from *Mycobacterium tuberculosis* mediates peptidyl-tRNA release and ribosome recycling in *Escherichia coli.* EMBO J. **20**, 2977–2986
23 Ito, K., Fujiwara, T., Toyoda, T. and Nakamura, Y. (2002) Elongation factor G participates in ribosome disassembly by interacting with ribosome recycling factor at their tRNA-mimicry domains. Mol. Cell **9**, 1263–1272
24 Guo, P., Zhang, L. Q., Qi, Z., Chen, R. S. and Jing, G. Z. (2005) Expression in *Escherichia coli*, purification and characterization of *Thermoanaerobacter tengcongensis* ribosome recycling factor. J. Biochem. (Tokyo) **138**, 89–94
25 Sambrook, J., Fritsch, E. F. and Maniatis, T. (1989) Molecular Cloning: A Laboratory Manual, Cold Spring Harbor Laboratory Press, Cold Spring Harbor, NY
26 Zhang, X. L., Guo, P. and Jing, G. Z. (2003) A vector with the downstream box of the initiation codon can highly enhance protein expression in *Escherichia coli*. Biotech. Lett. **25**, 755–760
27 Bao, Q., Tian, Y., Li, W., Xu, Z., Xuan, Z., Hu, S., Dong, W., Yang, J., Chen, Y., Xue, Y. et al. (2002) A complete sequence of the. *T tengcongensis* genome. Genome Res. **12**, 689–700
28 Ichikawa, S. and Kaji, A. (1989) Molecular cloning and expression of ribosome releasing factor. J. Biol. Chem. **264**, 20054–20059
29 Zengel, J. M., Archer, R. H. and Lindahl, L. (1984) The nucleotide sequence of the *Escherichia coli fus* gene coding for elongation factor G. Nucleic Acids Res. **12**, 2181–2192
30 Horton, R. M., Cai, Z., Ho, S. N. and Pease, L. R. (1990) Gene splicing by overlap extension: Tailor-made genes using the polymerase chain reaction. Biotechniques **8**, 528–535
31 Feng, Y. M., Zhang, Y. M. and Jing, G. Z. (2002) Soluble expression in *Escherichia coli,* purification and characterization of a human TF-1 cell apoptosis-related protein TFAR19. Protein Exp. Purif. **25**, 323–329
32 Zhou, B. and Jing, G. Z. (1998) Determination of protein extinction coefficients by alkaline hydrolysis. Progr. Biochem. Biophys. **26**, 384–387
33 Tai, P. and Davis, B. (1979) Isolation of polysomes free of initiation factors. Methods Enzymol. **59**, 362–371
34 Jelenc, P. C. (1980) Rapid purification of highly active ribosomes from *Escherichia coli*. Anal. Biochem. **105**, 369–374
35 Hirashima, A. and Kaji, A. (1972) Factor-dependent release of ribosomes from messenger RNA: requirement for two heat-stable factors. J. Mol. Biol. **65**, 43–58

36 Ohnishi, M., Janosi, L., Shuda, M., Matsumoto, H., Terawaki, T. and Kaji, A. (1999) Molecular cloning, sequencing purification and characterization of *Pseudomonas aeruginosa* ribosome recycling factor. J. Bacteriol. **181**, 1281–1291
37 Hirokawa, G., Kiel, M. C., Muto, A., Selmer, M., Raj, V. S., Liljas, A., Igarashi, K., Kaji, H. and Kaji, A. (2002) Post-termination complex disassembly by ribosome recycling factor, a functional tRNA mimic. EMBO J. **21**, 2272–2281
38 Janosi, L., Shimizu, I. and Kaji, A. (1994) Ribosome recycling factor (ribosome releasing factor) is essential for bacterial growth. Proc. Natl. Acad. Sci. U.S.A. **91**, 4249–4253
39 Janosi, L., Mottagui-Tabar, S., Isaksson, L. A., Sekine, Y., Ohtsubo, E., Zhang, S., Goon, S., Nelken, S., Shuda, M. and Kaji, A. (1998) Evidence for *in vivo* ribosome recycling, the fourth step in protein biosynthesis. EMBO J. **17**, 1141–1151
40 Fujiwara, T., Ito, K., Nakayashiki, T. and Nakamura, Y. (1999) Amber mutations in ribosome recycling factors of *Escherichia coli* and *Thermus thermophilus*: evidence for C-terminal modulator element. FEBS Lett. **447**, 297–302
41 Yamami, T., Ito, K., Fujiwara, T. and Nakamura, Y. (2005) Heterologous expression of *Aquifex aeolicus* ribosome recycling factor in *Escherichia coli* is dominant lethal by forming a complex that lacks functional co-ordination for ribosome disassembly. Mol. Microbiol. **55**, 150–161

Received 11 May 2005/20 October 2005; accepted 21 October 2005
Published as BJ Immediate Publication 21 October 2005, doi:10.1042/BJ20050780

42 Rodnina, M. V., Savelsbergh, A., Katunin, V. I. and Wintermeyer, W. (1997) Hydrolysis of GTP by elongation factor G drives tRNA movement on the ribosome. Nature (London) **385**, 37–41
43 Agrawal, R. K., Penczek, P., Grassucci, R. A. and Frank, J. (1998) Visualization of elongation factor G on the *Escherichia coli* 70 S ribosome: the mechanism of translocation. Proc. Natl. Acad. Sci. U.S.A. **95**, 6134–6138
44 Wilson, D. N., Schluenzen, F., Harms, J. M., Yoshida, T., Ohkubo, T., Albrecht, R., Buerger, J., Kobayashi, Y. and Fucini, P. (2005) X-ray crystallography study on ribosome recycling: the mechanism of binding and action of RRF on 50S ribosomal subunit. EMBO J. **24**, 251–260
45 Gao, N., Zavialov, A. V., Li, W., Sengupta, J., Valle, M., Gursky, R. P., Ehrenberg, M. and Frank, J. (2005) Mechanism for the disassembly of the posttermination complex inferred from cryo-EM studies. Mol. Cell **18**, 663–674
46 Ishino, T, Atarashi, K., Uchiyama, S., Yamami, T., Saihara, Y., Yoshida, T., Hara, H., Yokose, K., Kobayashi, Y. and Nakamura, Y. (2000) Interaction of ribosome recycling factor and elongation factor EF-G with *E. coli* ribosomes studied by the surface plasmon resonance technique. Genes to Cells **5**, 953–963